machines

MDPI

Review

On the Lightning Attachment Process of Wind Turbine–Observation, Experiments and Modelling

Zixin Guo [1,2], Wah Hoon Siew [3,*], Qingmin Li [4] and Weidong Shi [1,2]

[1] China Electric Power Research Institute, Beijing 100192, China; guozixin@epri.sgcc.com.cn (Z.G.); wdshi@epri.sgcc.com.cn (W.S.)
[2] Xizang Yangbajing High Altitude Electrical Safety & Electromagnetic Environment National Observation and Research Station, Lhasa 851517, China
[3] Department of Electronic & Electrical Engineering, University of Strathclyde, Glasgow G1 1XW, UK
[4] School of Electrical and Electronic Engineering, North China Electric Power University, Beijing 102206, China; lqmeee@ncepu.edu.cn
* Correspondence: wh.siew@strath.ac.uk

Abstract

Wind power plays an increasingly important role in power generation as one of the most popular renewable energy sources. With the increasing capacity and height of wind turbines, lightning incidents have become one of the most serious threats to wind turbines, especially for wind turbine blades. It is important to fully understand the lightning attachment process of a wind turbine, which is not only essential to academic research but also useful to the design of a lightning protection system. Plenty of work has been conducted from three main perspectives: field observations, laboratory experiments, and simulation models. In this paper, the existing research achievements have been reviewed, and problems to be solved have been proposed. The monitoring of lightning incidents on wind farms remains a challenge, and a device to capture lightning strikes to wind turbines with high efficiency is in demand. The impact of sensors on the blade on the lightning protection system cannot be ignored and needs further investigation. For the simulation model, the influence of space charge on the lightning attachment process is not fully understood, and improvements might be made to the existing model.

Keywords: wind turbine; lightning attachment; lightning protection

check for updates

Academic Editor: Francesco Castellani

Received: 9 June 2025
Revised: 7 August 2025
Accepted: 7 August 2025
Published: 9 August 2025

Citation: Guo, Z.; Siew, W.H.; Li, Q.; Shi, W. On the Lightning Attachment Process of Wind Turbine–Observation, Experiments and Modelling. *Machines* **2025**, *13*, 704. https://doi.org/10.3390/machines13080704

Copyright: © 2025 by the authors. Licensee MDPI, Basel, Switzerland. This article is an open access article distributed under the terms and conditions of the Creative Commons Attribution (CC BY) license (https://creativecommons.org/licenses/by/4.0/).

1. Introduction

Wind power is currently one of the most popular renewable energy sources. The latest data from the Global Wind Energy Council (GWEC) indicate that the global total installed capacity of wind turbines has exceeded 1021 GW by 2023 [1]. This figure comprises 946 GW of onshore capacity and 75 GW of offshore capacity. In China, the total installed capacity of wind power is 467 GW, representing the third largest source of energy after thermal power (1170 GW) and photovoltaic power (714 GW). In the United Kingdom, the generation of electricity from wind power has overtaken that from fossil fuels in a single quarter, becoming the largest single source of electricity.

The rapid construction of wind farms has led to an increase in the incidents of lightning strikes on wind turbines. The wind farms are usually situated in open and flat locations, and the wind turbines represent tall objects, which makes the wind farm particularly susceptible to lightning strikes. Statistical data indicate that lightning-related incidents represent over 60% of all natural disasters occurring in wind farms, posing a significant risk

to the safe and reliable operation of these facilities. Approximately one-third of lightning-related incidents result in direct damage to the wind turbine, while two-thirds are caused by induced lightning and subsequent damage to the electrical equipment. Blade damage accounts for 7% to 10% of all lightning accidents, control system damage accounts for 43% to 51%, and electrical system damage accounts for 20% to 32% [2]. Long-term statistics from different countries demonstrate that the rate of lightning strike damage to wind turbine blades is increasing annually, as illustrated in Table 1.

Table 1. Wind Turbine Lightning Damage Frequency.

Country	Year	Average Unit Capacity (MW)	Faults Per 100 Turbine Years
Denmark [3]	1990–1998	0.24	3.9
Japan [4]	2001–2004	1.65	6.2
US [5]	2009–2013	2.0	11.9
China [6]	2012–2017	≥1.5	9.8

As the capacity of wind turbine generators (WTG) increases, the size of the blades is also increasing, which will exacerbate the problem of lightning strikes. From the 1980s to the present, the tip height of onshore WTGs has increased from the initial 25.5 m to 245 m, while the rotor diameter has increased from 15 m to more than 220 m. The height of offshore WTGs is even more substantial, with the tip height exceeding 300 m and rotor diameter exceeding 280 m [1]. The increase in the size of WTGs, especially the size of the blades, presents three challenges to the lightning protection of wind turbines. Firstly, the increases in the size of WTGs result in a change in the form of lightning strikes on wind turbines. For WTG of a lower height, the predominant form of lightning strike is downward. However, for WTGs higher than 100 m, the main form of lightning strike is upward [7,8]. Secondly, the increase in the size of the blade results in a change in the material of the blade. For example, the main beam changes from insulating material glass fiber reinforced polymer (GFRP) to a relatively conductive carbon fiber reinforced polymer CFRP which faces much more risk of lightning strikes [9–11]. This subsequently leads to a significant change in the design of the lightning protection system (LPS) of CFRP blades. Thirdly, it is also unclear whether the LPS that is applicable to smaller-sized blades is still applicable to larger-sized blades. The typical structure of a wind turbine blade and its LPS is shown in Figure 1.

Furthermore, offshore wind turbines are susceptible to the issue of salt spray adhesion, which has the potential to impair the conductivity of the blade surface and consequently impact the interception efficiency of LPS [12].

Additionally, the phenomenon of wind turbine ice cover is emerging as a significant concern. The installation of electrothermal de-icing devices results in alterations to the electrical structure of the blade, leading to an increased possibility of lightning strikes.

Besides, the structure and operation conditions of WTG will also influence the electromagnetic field when the wind turbine blade is hit by lightning strikes. The reflection of lightning current along the WTG is different for the first return-stroke and subsequent return-strokes [13,14], which may influence the equipment and its protection system inside the nacelle.

To solve the problems mentioned above, it is important to study the lightning attachment process of wind turbine blades, including field observation, experimental work, and simulation models. It is essential to obtain the data of WTG lightning incidents and then recreate the conditions by laboratory experiments to evaluate the efficiency of LPS of wind turbine blades according to IEC standard 61400-24 [15]. Finally, construct a simulation model to analyze the lightning protection zone of wind turbine LPS [16–23]. This work

provides a critical review of current research in the lightning attachment process of wind turbines, identifying their limitations and proposing future research directions.

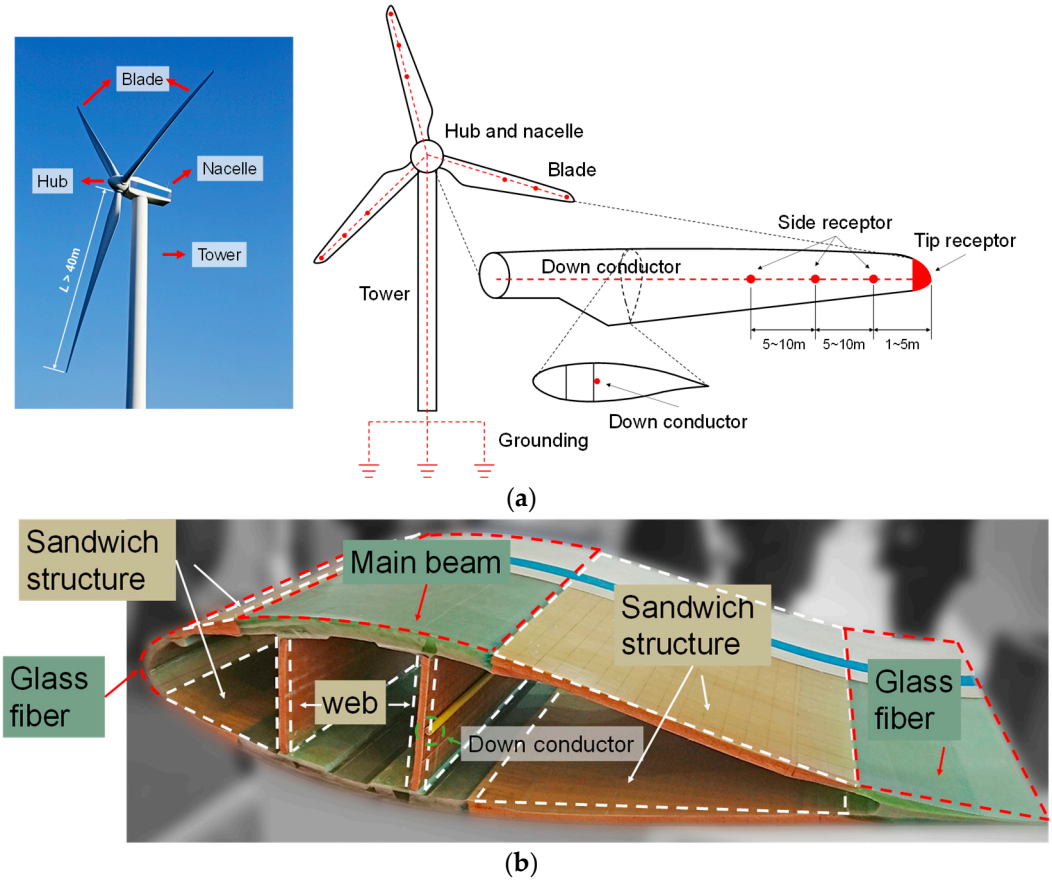

Figure 1. The typical structure of a wind turbine blade and its LPS. (**a**) The structure of the wind turbine blade and its LPS. (**b**) The cross-section of a wind turbine blade.

The paper is organized as follows. Section 2 presents the field observation results of lightning strikes to the wind turbine. Section 3 presents the experimental work related to the lightning attachment manner to the wind turbine. Section 4 presents the existing model of the Lightning Attachment Process of Wind Turbines. The summary of this work is presented in Section 5.

2. Field Observation of Lightning Strikes to Wind Turbine

The most effective method to obtain first-hand information about the lightning attachment process of WTG is through field observation. Researchers have conducted long-term observation of lightning strikes on wind turbines and obtained records including optical images, current waveforms, electric field waveforms, etc. The characteristics of wind turbine blade damage due to lightning strikes have been reported.

2.1. Statistics and Damage Patterns of Lightning Strikes on Wind Turbine Blades

Lightning strikes can cause severe damage to wind turbine blades, including blade rupturing or burnout, which will lead to the WTG being out of operation. Besides, other kinds of damages caused by lightning, such as tearing at the blade edge, cracking on the surface, will influence the normal operation of WTGs and need to be repaired immediately or as soon as possible. The data collected from field observation indicate that despite equipping with LPS, lightning incidents on blades occur with considerable frequency. Throughout the lifetime of a blade, it will inevitably suffer several lightning strikes, resulting in significant

lightning protection issues. A five-year observation of wind farms in Texas and Illinois indicates that with a total of 508 WTGs, on average, each WTG experienced blade damage due to lightning every 8.4 years. In other words, each WTG may suffer 2–3 blade damage incidents during its lifetime [5]. This analysis was based on 304 lightning-caused wind turbine blade damage incidents that required significant repair. The data from the Nikaho wind farm in Japan revealed that six fixed cameras installed in the wind farm recorded 152 cloud-to-ground flashes (CGs) in one single year; 128 of 152 lightning strikes directly struck WTGs. It is reported that several WTGs were struck multiple times a year, one of the WTGs being struck 20 times. Besides, there were 23 cloud-to-ground flashes that hit more than 2 WTGs. Yasuda et al. [24–26] collected a substantial number of blade damage incidents caused by lightning strikes and classified them into four categories. Level 1 is catastrophic damage that requires WTG shutdown immediately, including blade rupturing, blade burnout, and wire melting. Level 2 is serious damage that requires repair immediately, including cracking along the bond weld and tearing at the blade edge. Level 3 is normal damage that requires repair, including surface stripping and receptor loss. Level 4 is minor damage that may not be repaired, including receptor vaporization, surface scorching, and other minor damages. However, because of the limitation of observation methods, the field observation was unable to provide a record of the lightning attachment process to WTG where LPS fails to intercept the downward lightning leader. All the observation mentioned above indicates a simple but important question: why can the wind turbine blade be damaged even when equipped with LPS, which passed the test according to IEC standard 61400-24 [15]?

2.2. The Distribution of Lightning Striking Points on Wind Turbine Blades

To answer the question of why LPSs fail to protect wind turbine blades, more specific investigations of the distribution of lightning striking points have been reported. The statistical data indicate that most lightning strikes on wind turbine blades occur within 10 m of the blade tip. Vestas conducted a two-year field observation recording the lightning incidents of 236 39 m-blade. It is reported that 88% of the lightning strikes occurred within 1 m from the tip, with the remaining 12% within 4 m [27]. In a study conducted by Garolera [28], the location of lightning strikes on blades with an average length of approximately 35 m was recorded. Garolera analyzed the distribution of 304 lightning striking points on wind turbine blades. The investigation indicates that over 60% of the lightning strikes occurred within 1 m of the blade tip, over 90% occurred within 4 m of the blade tip, and all the strikes were located within 10 m of the blade tip. China Electric Power Research Institute collected the operational data of four wind farms in Yunnan, Guizhou, and Shanxi provinces over a period of three years, including 1332 wind turbines. The static data illustrate that 34% of the lightning striking points are located within 1 m of the blade tip, 75% within 2 m, and 93% within 4 m, as shown in Figure 2. For wind turbine blades up to 50 m in length, the sections most vulnerable to lightning strikes are located within 5 m from the blade tip, approximately 10~12% of the blade length. The location of lightning striking points is near the tip of the blade, while the receptor, which works as an air terminal of LPS, is also located near the very tip of the blade. For some incidents, the attachment point is only tens of centimeters away from the receptor. The tip area of the wind turbine blade should have good protection afforded by the receptors, as the receptors play the same role as a Franklin rod for buildings. So, the reason why LPS interception failure happens is not yet fully understood. One possible reason is that the LPS and wind turbine blade body are integrated together, which is different from the Franklin rod and protected structure. In this way, the shape of the LPS component does influence the electric field, not only for the inception efficiency of LPS but also for the possibility of unintended

attachment points on the blade surface. For example, the boundary of the tip receptor is a vulnerable position to be hit by lightning strikes. A typical arrangement of receptors can be seen in Figure 3.

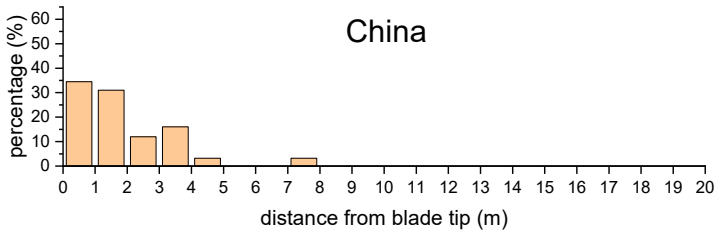

Figure 2. The distribution of lightning-strike direct-induced damage along the wind turbine blade, statistics from China.

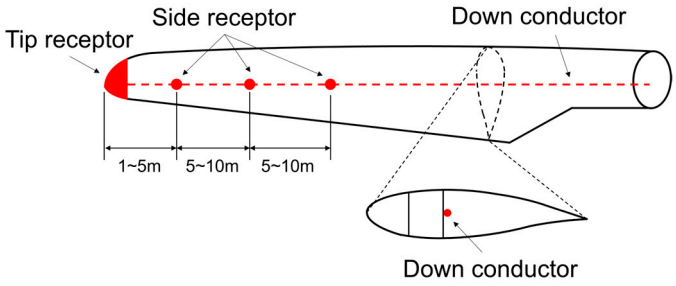

Figure 3. The typical arrangement of receptors along a wind turbine blade [29].

2.3. The Type and Characteristics of Lightning Discharge to Wind Turbine Blades

Because of the height and rotating operation condition of WTG, wind turbines are vulnerable to upward lightning discharge, and the rotating wind turbines are more likely to be struck than the stationary ones [30–33], as shown in Table 2.

Table 2. The Proportion of Upward Lightning Flashes to Wind Turbine Blades by Optical Observation.

No.	Proportion	Size of Observation Cases	Height of WTG	Location of Wind Farm	Reference
1	94%	36	100 m	Japan	[7,8]
2	43%	7	125 m	United States	[30]

For the reason that the lightning detection network may not detect upward lightning flashes as efficiently as downward lightning flashes, only optical observation results are taken into consideration here.

For wind turbines above 1.5 MW with a height of more than 100 m, upward lightning is the main type of lightning incident. Wang et al. [7,8] conducted an observation of lightning strikes on a 100 m WTG and a 45 m-nearby 105 m tower in Uchinada-chou. By 2010, a total of 36 lightning strikes on wind turbine blades were recorded, and 94% of those were upward lightning. Garolera [28] employed the U.S. National Lightning Detection Network (NLDN) to monitor lightning activity on wind turbine blades at a wind farm. Their findings revealed that among the lightning strikes observed on the blades, 50.1% were negative CGs, 15.3% were positive CGs, and 13.0% were upward lightning. The remaining 21.6% were not detected by the monitoring network. It is noted that the NLDN may not detect all upward lightning flashes because some of the upward lightning flashes exhibit different characteristics from downward ones, for example, some of the upward lightning does not have a return stroke but continuing current [30]. Wilson et al. [30] observed lightning strikes in a wind farm in Kansas and reported that 3 of 7 lightning-induced blade damages were caused by upward lightning. Cai et al. [34] conducted a long-term

observation study on a wind farm in Zhangbei, where he discovered that as many as 21 upward leaders initiated from different wind turbines. There is competition between different upward leaders from different wind turbines. Compared with downward CGs, upward CGs are dominated by discharges initiated from wind turbine blades instead of downward lightning leaders. For this scenario, the efficiency of upward leader inception from the receptor is extremely important in order to design and improve the existing lightning protection system. However, the existing design is far away from this demand, as shown by laboratory tests according to Standard [15]. During normal operation, wind turbines are in a rotating state. Montanyà et al. [31] conducted an observation in a wind farm with a 3-D Lightning Mapping Array and high-speed video. The results indicate that upward connecting leaders are easier to initiate from a rotating wind turbine blade. Therefore, reducing the speed of wind turbines can reduce their probability of being struck by lightning. Ishii et al. [32] conducted a five-year observation of 12 wind turbines in a wind farm off the coast of Japan. The findings indicated that when the blade angle exceeded 30° from vertical, the rotating blades were more likely to be struck by lightning discharge than static ones. Besides, all the lightning striking points are located at the tip of the blade. Wu et al. [35] made an observation of a wind turbine and a nearby tower using a lightning mapping array (LMA) observation. He reports that there is periodic discharge on the top of the wind turbine, and the period is related to the speed of the wind turbine blade. The power and height of discharge caused by WTG are much larger than those caused by a tower of similar height. Miki et al. [36] observed that when the blade is rotating upwards, there is an increased probability of initiating an upward leader, which may finally develop into CG. This phenomenon may be attributed to the distortion of the space charge generated by the corona near the blade due to rotation, which may facilitate the initiation of an upward leader. It is interesting to note that the distortion of space charge caused by the relative movement of the blade tip may lead to the discharge channel propagating towards the direction of rotation [37].

Whether the rotation of a wind turbine blade will enhance or reduce the probability of being struck by lightning remains unclear, based on both observation and experiments mentioned in Section 3, which is essential for a wind farm to choose the strategy during thunderstorms. For example, if the rotation increases the probability of the blade being struck by lightning, the operation strategy should dictate a stop in wind turbine operation during a thunderstorm. It is reasonable to believe that rotation will enhance the probability of initiation of upward leader from the wind turbine blade, which is very similar to the scenario of artificial initiation of lightning by rocket-and-wire triggering. The mechanism of rocket-wire-triggered lightning is that it creates a rapid change of electric field at the tip of the rocket to initiate an upward leader at the speed of about 200 m/s [38]. The speed of the wind turbine blade (>100 m/s) tip is comparable to that of rocket-wire-triggered lightning (~200 m/s).

2.4. The Monitoring of Lightning Current Parameters

The waveform of lightning current when a wind turbine blade is struck is related to the type of lightning discharge. For downward lightning, the amplitude of peak current is relatively large with a short duration. The current peak value can reach dozens or even hundreds of kA, and the duration generally does not exceed several milliseconds. For upward lightning, the amplitude of peak current is relatively small with a long duration. The current peak value is typically in the range of a few kA to a dozen kA, and the duration may be longer than hundreds of milliseconds [39–42].

The amount of charge for a single cloud-to-ground flash is generally no more than 100 C for downward lightning, while for upward lightning, the duration is 1–2 orders of

magnitude longer than that of downward lightning, which leads to a much larger amount of charge transferred. For example, the lightning incident data for wind turbines obtained by the Japan Electric Power Central Research Institute over a four-year monitoring period revealed that the charge transferred by all the recorded upward lightning strikes exceeded 100 C, with the highest reaching 687 C [43]. The IEC61400-24 recommends that the threshold value that wind turbine blades can withstand is 300 C [15]. The damage degree of wind turbine blades may be directly related to the amount of lightning transfer charge. The larger the charge transferred, the longer the lightning arc lasts, and the stronger the effects of it. For a lightning strike with a relatively small amount of charge transferred, hitting a wind turbine blade, it may cause blade surface scorching. However, for a large amount of charge transferred, it may cause the blade to explode [44].

There are nearly no reports on the charge magnitude of lightning strikes to wind turbine blades and their correlation with the kinds of damage. Taking the shielding failure of transmission lines as an example, it is well known that lightning strikes with relatively small current magnitude will cause shielding failure to a transmission line, because the upward leader initiating from the overhead ground wire fails to compete successfully with that from a phase line during the attachment process. However, for the wind turbine blade, the striking points on the blade surface are quite close to the receptor (decimeters), which cannot be explained by the shielding failure of the transmission line (meters). Besides, the overhead ground wire can be regarded as a separate part from the phase line because they are on a different crossarm of the transmission line tower and is insulated by an insulator. For a wind turbine blade, the receptors are part of the blade body. Under this condition, the blade body may be damaged even when the receptor intercepts a downward leader successfully by means of flashover or so.

Consequently, the monitoring of lightning current parameters is important to the analysis of lightning incidents affecting wind turbine blades, and the analytical techniques need to be improved.

3. Experimental Work on Lightning Attachment Manner to Wind Turbine

Experiments with long sparks play an important role in simulating the lightning attachment process of a wind turbine. Much work has been conducted to improve the method to simulate the lightning attachment process in a proper way, which involves not only the dimension of the test specimen, the choice of electrode configuration, but also the selection of waveforms, the length of the spark, etc.

3.1. Test Specimen

The length of a small-capacity wind turbine blade is relatively short, typically under 50 m or less. Most of the lightning strike points are located within 5 m of the blade tip. So, earlier studies used 3–5 m blade tip samples to conduct lightning attachment experiments [45–51]. As wind turbine capacity increases, blade length extends to be more than 100 m, which makes it insufficient to use the blade tip sample to simulate real operation conditions. So, researchers started to employ scale wind turbines for experiments [52–54]. The ratio of scale wind turbine is about 1:40 or so, and the real length of the scale blade ranges from 1.5 m to 2 m. The linear speed of the blade tip is similar to the real one (~100 m/s and larger); however, the angular speed is much faster, about 20 times higher or so. Besides, the space near the scaled model blade tip is relatively smaller than the real wind turbine blade, which may bring unexpected differences when taking space charge into consideration. The attachment manner under a scale wind turbine is similar to a real wind turbine in some respects, and some of the results are shown in Section 3.5.

In addition, the material used for the main beam of the blade does influence the design of LPS. For blade lengths larger than 100 m, the carbon fiber reinforced polymer (CFRP) is used instead of glass fiber reinforced polymer (GFRP). The conductivity of CFRP has a negative impact on the efficacy of the conventional LPS adopted for GFRP blades [9,10]. The method to protect CFRP blades from side flashes (or inboard flashes) needs to be further investigated.

3.2. Electrode Configuration

To simulate the lightning attachment process, both the plane electrode and rod electrode are employed for different purposes, as shown in Figure 4. Besides, an arc-shaped electrode is also used in experiments, which is similar to a plane electrode [52]. The plane electrode is used to focus on the process of upward leader initiation from wind turbine blades. The electric field generated by a plane electrode is believed to be similar to that by a downward leader [27,48].

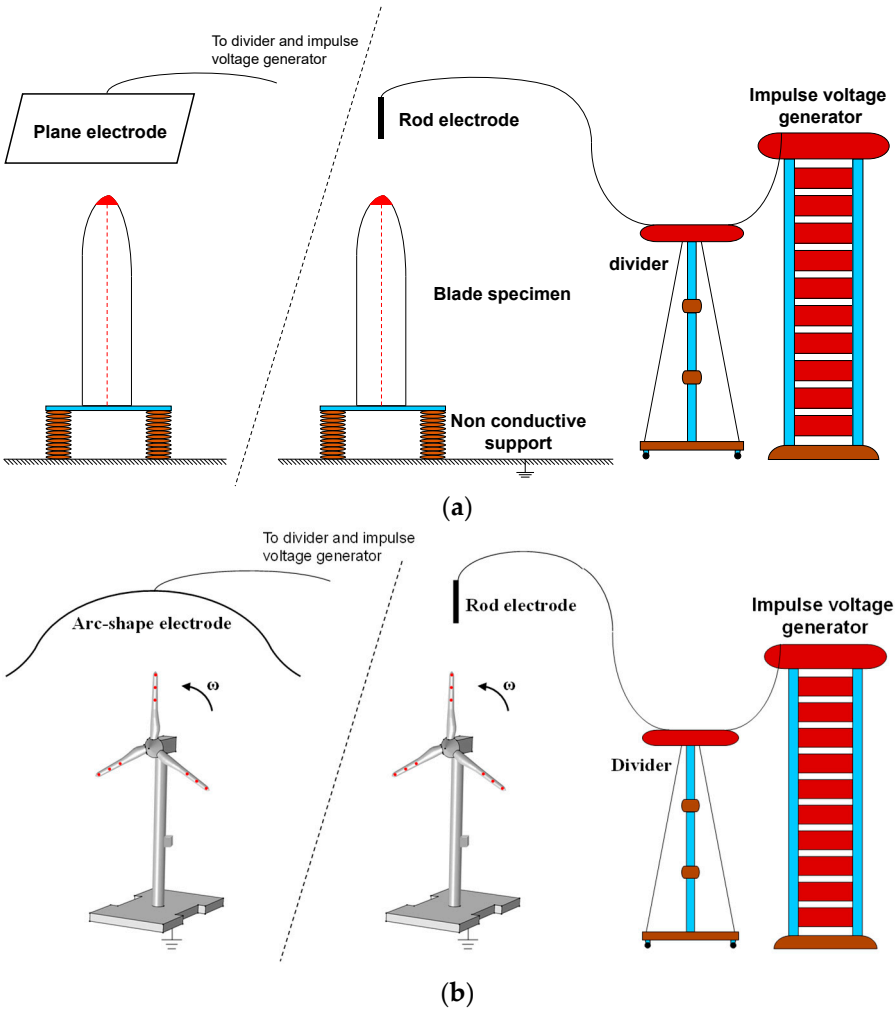

Figure 4. The schematic of the wind turbine blade lightning attachment experimental setup using different kinds of electrode configurations. (**a**) plane electrode and rod electrode for the real blade specimen. (**b**) An arc-shaped electrode and a rod electrode for a scale wind turbine.

The rod electrode is used to investigate the attachment process between the downward leader and the upward connecting leader. The leader can develop from a rod electrode upward to a blade, and the connecting process is simulated by this configuration [45–47,55]. Besides, an arc-shaped electrode is also introduced to conduct long-spark experiments,

which is similar to the plane electrode [52,54,56]. In IEC 61400-24, a plane electrode is recommended [15].

However, the length of the air-gap used in existing experimental work is limited to 10 m or so because of the designed capability of the equipment, which is much smaller in scale than natural lightning. For example, the typical length of a step for a stepped downward leader is 10 m. The process of natural lightning attachment, such as the upward leader from a tall building failing to connect with the downward leader and with the downward leader striking the side of the structure, is hard to reproduce in a laboratory. On the other hand, the real electric field when an upward leader initiates from a wind turbine blade is the combination of both a relative static field generated by the thundercloud and a transient field generated by downward leader propagation. However, most of the experiments conducted in the laboratory employ only the transient electric field. The difference between experimental work and natural lightning attachment process should not be forgotten, and its influence on the performance of LPS should be evaluated accordingly.

3.3. The Selection of Waveform

It is reported that the electric field generated by a 250/2500 μs switching impulse is more similar to that of real lightning discharge [57]. It is noted that the lightning impulse in high voltage experiments is used to describe the electric field caused by the return stroke, which is the process after lightning attachment has taken place. The lightning attachment process is a relatively slow process compared to the return stroke, where the attachment process lasts about 100 μs, and the return stroke lasts several μs. It is recommended by the standard IEC 61400-24 to use the standard switching impulse for testing [15]. Japanese researchers compare the lightning attachment process of a wind turbine blade under both lightning impulse and switching impulse, and the experimental results indicate that the possibility of receptor inception failure under lightning impulse is larger than that under switching impulse [45–47].

3.4. The Characteristics of Lightning Attachment Manner of Different Kinds of Blade Receptor

Different from the LPS for transmission line or tall buildings, such as Franklin rod or overhead ground wire (which are separate from the protected objects), the LPS of wind turbine blades consists of the receptor and down-conductor inside/outside the blade body. The main types of receptors include tip receptor, side receptor, metal mesh, metal stripe, etc. The down-conductor may be either a built-in or an external type conductor. The type, location, and number of receptors vary between different wind turbine manufacturers. To obtain the optimal protection effect, experimental work has been conducted to test the lightning attachment manner of different receptors.

In a study conducted by Vasa [45], 3 m-long blade tip specimens are used to compare the effects of lightning strikes on blades with and without receptors under different blade orientations. It is observed that while the receptor is effective in intercepting the lightning downward leader, the blade body remains struck by lightning discharge, and damage is caused.

Arinaga [46] compares the lightning attachment characteristics of the tip receptor and side receptor. It is reported that the lightning discharge may puncture the blade body at the very tip of the blade with only a side receptor, and the arc channel develops inside the blade chamber and causes damage, while the blade specimen with a tip receptor is well protected. The influence of the side receptor size on lightning attachment characteristics is also investigated.

Shindo et al. [16] conducted experiments with a 3 m specimen, which is cut from a 1 MW wind turbine blade equipped with a tip receptor and a side receptor. The lightning

interception efficiency of receptors under different blade orientations is evaluated. It is revealed that when the blade is 0 degrees horizontal, both tip and side receptors fail to intercept downward leader, and the upward leader initiates from the blade surface, which finally causes blade damage.

Muto et al. [49] discovers through experiments that the field strength is higher at the junction of the blade surface and tip receptor due to the shape of the tip receptor, which makes the junction area vulnerable to being struck by lightning discharge. Hence, he proposes adding insulation material at the junction area to reduce the distortion of fields.

Minowa et al. [55] points out that the stripes near the side receptor can provide an additional path for creeping discharge along the blade surface and increase the interception efficiency of the receptor.

Abd-Elhady et al. [50] compares the lightning attachment manner of metal mesh, external down-conductor, tip receptor, and side receptor. The performance of the metal mesh and external down-conductor is better than that of the tip and side receptor. Based on that, he proposes an improved design of LPS which combines the structure of metal mesh and external down-conductor.

Guo et al. [51] reports that the polarity of lightning discharge significantly influences the attachment manner of blade LPS, as shown in Figure 5. The destructive impact of positive lightning strikes is more pronounced than that of negative ones, and the interception failure of the receptor can be divided into three typical patterns. The qualitative mechanism of the polarity effect is as follows: the combined effect of the space charge generated by the corona discharge at the tip of the blade and the blade orientation hinders the initiation of the upward negative leader from the receptor, which promotes the development of creeping discharge along the blade surface and finally causes damage. Experimental work is also conducted to investigate the performance of metal mesh to protect the CFRP main beam [11]. The metal mesh has little influence on the attachment process. The metal mesh may provide extra protection on the condition that the lightning strike hits the blade surface directly when the receptor fails to intercept the downward leader.

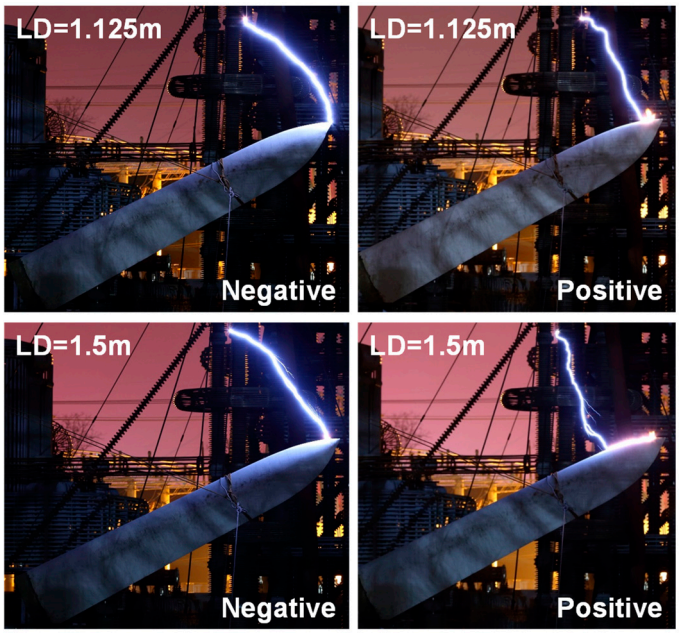

Figure 5. The lightning attachment manner under different polarity discharges [51].

He et al. [58] and He et al. [59] discusses the reason for blade puncture damage by lightning strikes. The conclusion can be reached that streamer discharge may initiate firstly from the down-conductor before the final jump and cause puncture damage.

Plenty of experimental work has been conducted to obtain the lightning attachment characteristics of a wind turbine blade. However, a critical problem of why receptors fail to protect a blade surface from lightning strikes is still not solved. Now we know that the position of the blade, the type of receptor equipped on the blade, and the polarity of lightning strikes influence the receptor interception efficiency. We have little knowledge about which factor or factors play the leading role in the lightning interception failure, for example, the type of lightning or the polarity, to name a couple. There are few reports about reproducing the incidents that caused damage to the wind turbine blade by lightning strikes in a laboratory. Maybe the polarity effect is part of the reason. Only when these two problems are resolved, it is possible to design a better LPS to protect wind turbine blades from lightning strikes.

3.5. The Influence of Blade Rotation on the Lightning Attachment Manner to the Blade

Radičević et al. [52] conducted experiments using a 1:40 scaled wind turbine model under a 2 m air gap to simulate the lightning attachment process of wind turbines in rotation. The experimental setup is shown in Figure 4b, left. The breakdown voltage increases when the rotation speed increases under this scenario. However, Wen et al. [54] found that when the length of the air gap increases, this phenomenon is reversed. He and his group use scaled wind turbines of a similar size and change the gap length from 1 m to 8 m. When the gap length is larger than 4 m, the breakdown voltage decreases as the rotation speed increases. We [53] compared the distribution of strike points of wind turbine blades in rotation under both positive and negative lightning conditions. It can be concluded that the rotation of the blade enhances the possibility of interception failure of positive lightning strikes and has little influence on negative lightning strikes. Two typical examples are shown in Figure 6. The influence of rotation on positive lightning is that a negative upward leader is relatively difficult to initiate from the receptor compared with a positive one. So, the time left for a negative upward connecting leader to intercept a downward leader is shorter than a positive one, which may cause receptor failure. The rotation is another difference from the lightning protection of a wind turbine blade to that of a transmission line or a tall building. However, the influence of rotation on the attachment process needs further investigation. Once the influence of rotation is finally determined, the strategy of wind turbine operation can be made during a thunderstorm.

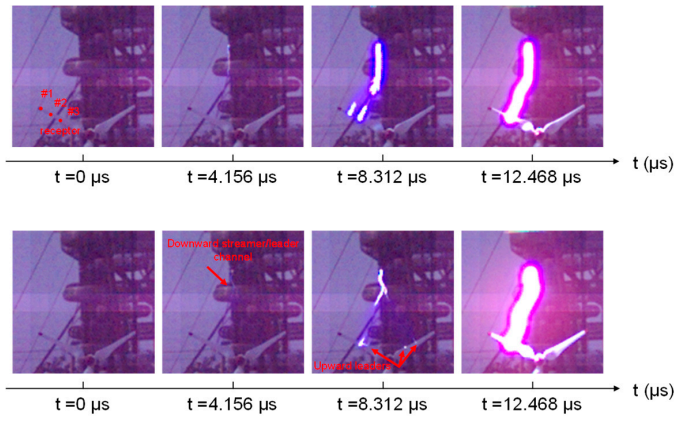

Figure 6. The rotation of the blade enhances the possibility of interception failure of positive lightning strikes. The #2 and #3 receptors intercept the downward leader instead of the #1 receptor for positive discharge under blade orientation larger than 45° [53].

3.6. The Influence of Surface Condition on Lightning Attachment Manner to Wind Turbine Blade

Li et al. [12] conduct experiments to compare the influence of salt water on the surface of wind turbine blades on the interception efficiency of LPS. The results indicate that saltwater can induce creeping discharge along the blade surface more easily than dry conditions, and the arc can develop into several channels and finally lead to more than one puncture point on the blade surface. Besides, the junction of the saltwater adhering area and the dry area is more vulnerable to lightning strikes.

Jiang et al. [60] investigated the influence of precipitation static on rotating wind turbine blades on lightning attachment characteristics. They measure the surface charge density of blades generated through friction with airborne particles. Compared with simulation results, it is concluded that the precipitation static on the rotating blade can reduce the electric field near the receptor to 38%, which will decrease the interception efficiency of LPS significantly. Besides, the precipitation static on rotating blades may develop into creeping discharge and cause damage to the blades.

For offshore wind farms, the surface condition of the wind turbine blade does influence the performance of LPS. However, further work needs to be conducted to quantitatively evaluate the influence of the marine environment on the performance of LPS and how to maintain it. It is possible to use a hydrophobic coating for offshore wind turbine blades, which is used to protect blades from icing in laboratory tests [61].

4. Model of Lightning Attachment Process of Wind Turbine

The accuracy of lightning shielding analysis depends on the model of the lightning attachment process, which is the foundation of evaluating the efficiency of LPS. The lightning attachment process is a complicated physical procedure, so the model has gone through a development process from simple to complex.

4.1. From Electro-Geometrical Model to Leader Progression Model

The lightning protection for wind turbine blades is similar to that for transmission lines, distribution lines, and buildings, which goes through a process from electro-geometrical model (EGM) to leader progression model (LPM). The literature about EGM and LPM can be found in [62–66], and the comparison with EGM and LPM is illustrated in Table 3. The EGM is a simplified model to describe the attachment of a lightning strike to a grounded object. The striking distance is the key concept of EGM, which refers to the distance between the grounded object and the tip of the downward leader when the upward connecting leader initiates [67]. So, EGM ignores the competition of different upward leaders from different positions of grounded objects, and once the upward leader initiates from a particular position, it will finally be hit. There are some different definitions [68] of striking distance, which are not discussed here. However, for tall, grounded objects like a wind turbine, the electric field distortion is much stronger, and the upward leader initiating and propagating process is more obvious and cannot be ignored. There may be competition between upward leaders from different receptors of one single blade or different blades or even the blade surface. That is the reason why LPM is introduced to analyze the lightning attachment manner of wind turbines. The LPM takes not only the descent of the downward leader but also the inception of upward leaders from grounded objects during the movement of the downward leader. So, the LPM accords more perfectly with physical reality.

Table 3. The comparison with EGM and LPM.

	EGM	LPM
Physical process involved	The initiation of upward leader	The propagation of downward leader, the initiation and development of upward leader, the competition of different upward leader during attachment process
Variables	Peak value of current, structure of grounded objects	Peak value of current, structure of grounded objects, speed of downward leader, property of leader channel
The complexity of calculation	Easy (striking distance is define by peak value of current)	Complicated (Involved calculation of electric field)
Typical method	Rolling sphere method	SLIM
Application	Widely used for lightning protection design of grounded objects, e.g., transmission line, wind turbine	Mainly used in academic research

Shindo et al. [16] proposed a model to compute the distribution of lightning strike points on the blade based on EGM. In his work, a two-point model is used for thundercloud, and a branchless line charge with a uniform charge distribution is used for the downward leader. The strike point is determined when the distance between the downward leader and the blade is less than the striking distance. Madson et al. [17,18] developed a method to calculate the shielding effect of the receptor on the blade surface. The SLIM model proposed by Becerra and Cooray [66] is used to determine the initiation of the upward leader. The height of the downward leader is recorded as the attachment point when the upward leader initiates. Each point on the blade surface has an attachment point, and all the attachment points comprise a collection surface, which can be used to analyze the shielding effect of different blade receptors in different blade positions. An example of a collection surface is shown in Figure 7. Furthermore, Madsen [19] calculated the electric field near wind turbines in different locations in a wind farm, and he pointed out that wind turbines in particular locations are more vulnerable to lightning strikes. Zhang et al. [20] proposed a method to calculate the optimum distance between wind turbines for lightning protection purposes. Most of the research is focused on a particular point on the blade surface, such as the discrete receptors. However, it is more important to evaluate the lightning risk of the whole blade surface. We attempt to evaluate the lightning risk of blade surface by the following procedure: firstly, divide the blade surface into an array of points; secondly, calculate the moment when upward leader initiates from the chosen points for all the points under the same downward leader condition; finally draw the probability distribution of the whole blade surface according to the sequential order of upward leader inception, as shown in Figure 8 [29].

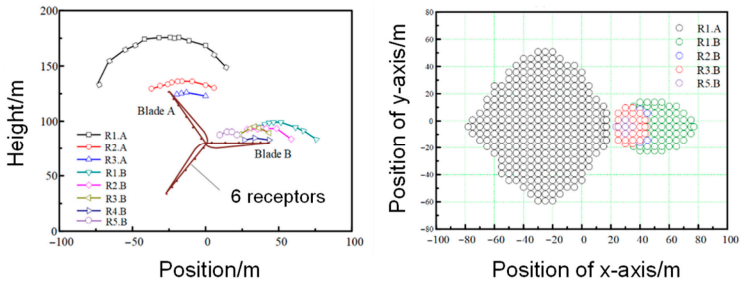

Figure 7. The example of the collection surface of a wind turbine blade with six side receptors.

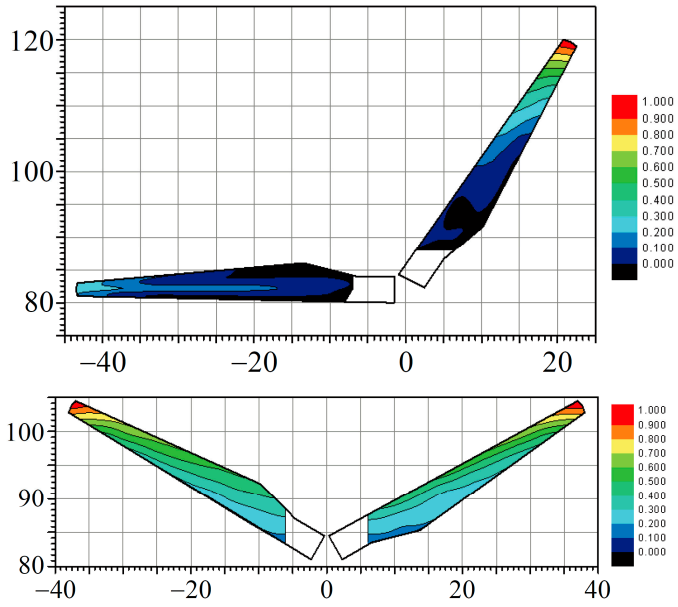

Figure 8. Lightning strike probability distribution of WT blade in 90°/30° from vertical, and 60°/60° from vertical position. The unit of the x and y axes is in meters [29].

The speed of different kinds of downward leaders has a significant influence on the interception efficiency of the blade receptor [69–71]. The average speed of downward leaders of the first stroke ranges from 1×10^5 to 8×10^5 m/s. However, the average speed of the dart leader of subsequent strokes is about 1×10^7 m/s, which is two orders of magnitude larger. The speed of the downward leader influences the time of upward connecting leader initiation from receptors. The critical length of the initial streamer that can satisfy the initiation of the upward leader is linearly related to the speed of the downward leader, and inversely proportional to the current peak with a constant offset [29]. So, the larger the speed of the downward leader, the shorter the striking distance, and the more likely the LPS may fail to intercept the downward leader. Based on the SLIM model, Long et al. [21,22] calculated the striking distance of the blade receptor under dart leader. The results indicate that the interception failure of the receptor depends on several factors, including the difference in downward leader speed, the position of the blade when lightning strikes, the interval between first and subsequent strokes, and the peak value of subsequent strokes. Nie et al. [23] analyzed the influence of terrain topography on the lightning shielding effect by using the SLIM model.

There are two questions remaining to be solved for the model of the attachment process of the wind turbine. Firstly, LPM cannot explain why lightning strikes hit the wind turbine blade surface instead of the receptors. When conducting LPM, the potential position of upward leader initiation is given by the researcher; for example, one can set the calculation procedure to simulate the upward leaders initiating from different receptors. It is impossible for the existing LPM model to simulate upward leaders initiating from random positions on the blade surface. Secondly, the existing LPM models are based on several semi-empirical and semi-experimental equations, which cannot simulate the real attachment process of a wind turbine precisely. Some tools based on EGM or LPM have been developed to help design the LPS of wind turbine blades. However, not all experimental work can be replaced by simulation models to date.

4.2. The Influence of Space Charge on the Model

Bazelyan et al. [72] calculated the corona initiation from grounded objects under thunderstorm conditions and pointed out that the space charge generated by corona can

restrain the inception of upward leaders from grounded objects and finally influence the attachment manner. However, Becerra [73,74] compared the leader initiation process from lightning rod with and without the corona induced space charge and reported that the protection area reduced about 10% when taking space charge into account, which is as dramatic as Bazelyan mentioned. Besides, the distribution of space charge can be disturbed easily by wind or rotation of the blade, as the vertical velocity of space charge is about 8 m/s. The observation of wind farms also confirmed this trend, where the upward lightning from wind turbines usually happened when the wind speed is lower than that from the tower nearby [75]. Yu et al. [76] calculated the distribution of space charge under a rotating wind turbine; the shape of the space charge cluster is influenced by the rotating speed, and the faster the blade rotates, the stronger the electric field near the blade is distorted by space charge.

There are still many conflicting conclusions about the influence of space charge on the lightning attachment manner of wind turbines, which need to be further investigated.

Taking field observation and experimental results into consideration, there is a gap between the existing model and real lightning strikes to the wind turbine blade. The LPS failure is still hard to simulate by existing models. The model that can simulate the process of both downward and upward lightning, for both negative and positive polarity, and with the influence of space charge due to blade rotation, may be the goal of further research in this topic. With this model, the performance of LPS can be tested and redesigned much efficiently and economically.

5. Summary

In this paper, we analyzed the challenges brought to the lightning protection of wind turbine blades with the changes in the capacity, size, and application scenarios of the WTG. The current research achievements on the lightning attachment process of WTG are summarized from three aspects: field observation, experimental work, and simulation model. Several issues that need further investigation are proposed.

The monitoring of lightning accidents on wind farms remains a challenge. The lack of comprehensive data for real cases of lightning incidents to wind turbine blades limits the improvement of the LPS for WTG. The existing monitor method is mainly based on a lightning detection system whose detection efficiency varies for different kinds of lightning, especially upward lightning. Besides, it is an indirect method compared with optical observation. So, a composite observational system including electromagnetic field, optical images of the lightning process, and the current waveform of lightning strikes hitting a wind turbine blade is in demand.

The experimental work faces the challenge of accurately replicating the conditions of real lightning strikes to WTGs, including the attachment manner under different polarities, with the influence of rotation, and so on. For blade rotation, it is necessary to break away from the conventional thinking of long air gap experiments, which use only switching or lightning impulse to simulate a lightning strike. Both the background electric field of thunderstorm (relatively static electric field) and the electric field induced by lightning leader (transient electric field) should be taken into consideration. Besides, the influence of space charge is a key factor to be involved.

A more comprehensive model of the lightning attachment process is in pressing demand, which is suitable for both downward and upward lightning strikes, under both positive and negative polarities. In this way, the mechanism of LPS failure can be discovered by simulation and experimental work.

Last but not least, the operation strategy can be optimized when all the above challenges are solved, including whether WTGs need to stop during a thunderstorm.

Author Contributions: Conceptualization, Z.G., writing—original draft preparation, Z.G.; writing—reviewing and editing, W.H.S.; supervision, Q.L. and W.S. All authors have read and agreed to the published version of the manuscript.

Funding: This research was funded by the National Natural Science Foundation of China under Grant 52207176.

Data Availability Statement: The raw data supporting the conclusions of this article will be made available by the authors on request.

Conflicts of Interest: The authors declare no conflicts of interest.

References

1. Global Wind Energy Council. *Global Wind Report 2024*; Global Wind Energy Council: Brussels, Belgium, 2024.
2. Glushakow, B. Effective lightning protection for wind turbine generators. *IEEE Trans. Energy Convers.* **2007**, *22*, 214–222. [CrossRef]
3. Cotton, I.; McNiff, B.; Soerenson, T.; Zischank, W.; Christiansen, P.; Hoppe-Kilpper, M.; Ramakers, S.; Pettersson, P.; Muljadi, E. Lightning protection for wind turbines. In Proceedings of the 25th International Conference on Lightning Protection (ICLP2000), Rhodes, Greece, 18–22 September 2000; pp. 848–853.
4. Wada, A. Lightning damages of wind turbine blades in winter in japan-Lightning observation on the nikaho-kogen wind farm. In Proceedings of the 27th International Conference on Lightning Protection (ICLP2004), Avignon, France, 13–16 September 2004; pp. 1–6.
5. Garolera, A.C.; Madsen, S.F.; Nissim, M.; Myers, J.D.; Holboell, J. Lightning damage to wind turbine blades from wind farms in the US. *IEEE Trans. Power Deliv.* **2014**, *31*, 1043–1049. [CrossRef]
6. Chen, W.; He, T.; Bian, K.; He, H.; Xiang, N.; Shi, W.; Li, X.; Zhang, S.; Sun, T.; Li, Z.; et al. Review of research on lightning damage and protection of wind turbine blades. *High Volt Eng.* **2019**, *45*, 1–15.
7. Wang, D.; Takagi, N.; Watanabe, T.; Sakurano, H.; Hashimoto, M. Observed characteristics of upward leaders that are initiated from a windmill and its lightning protection tower. *Geophys. Res. Lett.* **2008**, *35*, L02803. [CrossRef]
8. Wang, D.; Takagi, N. Typical characteristics of upward lightning observed in Japanese winter thunderstorm and their physical implications. In Proceedings of the 14th International Conference of Atmospheric Electricity, Rio de Janeiro, Brazil, 8–12 August 2011; pp. 1–5.
9. Harrell, T.M.; Madsen, S.F.; Thomsen, O.T.; Dulieu-Barton, J.M. On the Effect of Dielectric Breakdown in UD CFRPs Subjected to Lightning Strike Using an Experimentally Validated Model. *Appl. Compos. Mater.* **2022**, *29*, 1321–1348. [CrossRef]
10. Madsen, S.F.; Carloni, L. Lightning exposure of Carbon Fiber Composites in wind turbine blades. In Proceedings of the 24th Nordic Insulation Symposium on Materials, Components and Diagnostics, Copenhagen, Denmark, 15–17 June 2015.
11. Guo, Z.; Yu, W.; Fang, Z.; Zhang, M.; Li, H.; Li, Q.; Siew, W.H. The influence of the metal mesh to the attachment manner of CFRP wind turbine blades. In Proceedings of the 11th Asia-Pacific International Conference on Lightning (APL-2019), Hong Kong, China, 12–14 June 2019; pp. 1–4.
12. Li, Q.; Ma, Y.; Guo, Z.; Ren, H.; Wang, G.; Arif, W.; Fang, Z.; Siew, W.H. The Lightning Striking Probability for Offshore Wind Turbine Blade with Salt Fog Contamination. *J. Appl. Phys.* **2017**, *122*, 073301. [CrossRef]
13. Torchio, R.; Nicora, M.; Mestriner, D.; Brignone, M.; Procopio, R.; Alotto, P.; Rubinstein, M. Do Wind Turbines Amplify the Effects of Lightning Strikes? A Full-Maxwell Modelling Approach. *IEEE Trans. Power Del.* **2022**, *37*, 3996–4006. [CrossRef]
14. Torchio, R.; Nicora, M.; Mestriner, D.; Brignone, M.; Procopio, R.; Alotto, P.; Rubinstein, M. Full-Wave Analysis of Wind Turbine Transient Response to Direct Lightning Strikes. In Proceedings of the 17th International Symposium on Lightning Protection (SIPDA 2023), Suzhou, China, 9–13 October 2023.
15. *IEC 61400-24*; 2019 Wind Turbine Generator Systems—Part 24: Lightning Protection. IEC: Genève, Switzerland, 2019.
16. Shindo, T.; Asakawa, A.; Miki, M. A study of lightning striking characteristics to wind turbines. In Proceedings of the 29th International Conference on Lightning Protection (ICLP2008), Uppsala, Sweden, 23–26 June 2008; pp. 9c-4-1–9c-4-9.
17. Madsen, S.F.; Erichsen, H.V. Numerical model to determine lightning attachment point distributions on wind turbines according to the revised IEC 61400-24. In Proceedings of the International Conference on Lightning and Static Electricity (ICOLSE2009), Pittsfield, MA, USA, 15–17 September 2009; pp. 15–17.
18. Madsen, S.F.; Mieritz, C.F.; Garolera, A.C. Numerical tools for lightning protection of wind turbines. In Proceedings of the 2013 International Conference on Lightning and Static Electricity (ICOLSE2013), Seattle, WA, USA, 18–20 September 2013; pp. SEA13-2.1–SEA13-2.6.
19. Madsen, S.F. Interaction Between Electrical Discharges and Materials for Wind Turbine Blades-Particularly Related to Lightning Protection. Ph.D. Thesis, Technical University of Denmark, Lyngby, Denmark, 2006.

20. Zhang, L.; Lao, H.; Wang, G.; Zou, L.; Zhao, T.; Fang, Z. A new method for spatial allocation of turbines in a wind farm based on lightning protection efficiency. *Wind. Energy* **2019**, *22*, 1310–1323. [CrossRef]
21. Long, M.; Becerra, M.; Thottappillil, R. On the attachment of dart lightning leaders to wind turbines. *Electr. Power Syst. Res.* **2017**, *151*, 432–439. [CrossRef]
22. Becerra, M.; Long, M.; Schulz, W.; Thottappillil, R. On the estimation of the lightning incidence to offshore wind farms. *Electr. Power Syst. Res.* **2018**, *157*, 211–226. [CrossRef]
23. Nie, J.; Xiang, N.; Li, K.; Chen, W. Multiple wind turbines shielding model of lightning attractiveness for mountain wind farms. *Electr. Power Syst. Res.* **2023**, *224*, 109727. [CrossRef]
24. Yasuda, Y.; Yokoyama, S. Proposal of lightning damage classification to wind turbine blades. In Proceedings of the 7th Asia-Pacific International Conference on Lightning (APL2011), Chengdu, China, 1–4 November 2011; pp. 368–371.
25. Yasuda, Y.; Yokoyama, S.; Ideno, M. Classification of lightning damage to wind turbine blades. In Proceedings of the 31st International Conference on Lightning Protection (ICLP2012), Vienna, Austria, 16–20 September 2012; pp. 559–566.
26. Yokoyama, S.; Yasuda, Y.; Minowa, M.; Sekioka, S.; Yamamoto, K.; Honjo, N.; Sato, T. Clarification of the mechanism of wind turbine blade damage taking lightning characteristics into consideration and relevant research project. In Proceedings of the 31st International Conference on Lightning Protection (ICLP2012), Vienna, Austria, 16–20 September 2012; pp. 1–6.
27. Madsen, S.F.; Holbøll, J.; Henriksen, M.; Bertelsen, K.; Erichsen, H.V. New test method for evaluating the lightning protection system on wind turbine blades. In Proceedings of the 28th International Conference on Lightning Protection (ICLP2006), Kanazawa, Japan, 17–21 September 2006; pp. 1497–1502.
28. Garolera, A.C. Lightning Protection of Flap System for Wind Turbine Blades. Ph.D. Thesis, Technical University of Denmark, Lyngby, Denmark, 2014.
29. Guo, Z. The Polarity Effect of Lightning Attachment on Wind Turbine Blade and Risk Assessment Method. Ph.D. Thesis, North China Electric Power University, Beijing, China, 2020.
30. Wilson, N.; Myers, J.; Hutchinson, M. Lightning attachment to wind turbines in central Kansas: Video observations, correlation with the NLDN and in-situ peak current measurements. In Proceedings of the European Wind Energy Association, Vienna, Austria, 4–7 February 2013; pp. 284–291.
31. Montanyà, J.; Velde, O.; Williams, E.R. Lightning discharges produced by wind turbines. *J. Geophys. Res. Atmos.* **2014**, *119*, 1455–1462. [CrossRef]
32. Ishii, M.; Saito, M.; Natsuno, D.; Sugita, A. Lightning incidence on wind turbines in winter. In Proceedings of the 32nd International Conference on Lightning Protection (ICLP2014), Shanghai, China, 12–17 October 2014; pp. 1734–1738.
33. Alonso, M.A.; Irastorza, D.C. Dynamic Wind Turbine Lightning Protection Behaviour under Storm Conditions. In Proceedings of the 29th International Conference on Lightning Protection (ICLP2008), Uppsala, Sweden, 23–26 January 2008.
34. Cai, L.; Ke, Y.; Fan, W.; Yan, R.; Zhou, M.; Wang, J.; Fan, Y. Observation of an upward lightning flash with 21 upward positive leaders initiated from different wind turbines in wind farm. *High Volt.* **2024**, *9*, 163–171. [CrossRef]
35. Wu, T.; Wang, D.; Rison, W.; Thomas, R.J.; Edens, H.E.; Takagi, N.; Krehbiel, P.R. Corona discharges from a windmill and its lightning protection tower in winter thunderstorms. *J. Geophys. Res. Atmos.* **2017**, *122*, 4849–4865. [CrossRef]
36. Miki, M.; Miki, T.; Wada, A.; Asakawa, A.; Asuka, Y.; Honjo, N. Observation of lightning flashes to wind turbines. In Proceedings of the 30th International Conference on Lightning Protection (ICLP2010), Cagliari, Italy, 13–17 September 2010; pp. 1–7.
37. Wu, Q.; Wang, Y.; Du, Z.; Wu, Z.; Deng, Y.; Wen, X. Positive corona discharge of rod-plate electrodes in high-speed airflow. *High Volt.* **2024**, *10*, 337–350. [CrossRef]
38. Uman, M.A. *The Art and Science of Lightning Protection*, 1st ed.; Cambridge University Press: Cambridge, UK, 2008.
39. Rakov, V.A.; Uman, M.A. *Lightning: Physics and Effects*; Cambridge University Press: New York, NY, USA, 2003.
40. Weidman, C.D.; Krider, E.P. The fine structure of lightning return stroke waveforms. *J. Geophys. Res.* **1978**, *83*, 6239–6247. [CrossRef]
41. Diendorfer, G.; Pichler, H.; Mair, M. Some parameters of negative upward-initiated lightning to the Gaisberg Tower (2000–2007). *IEEE Trans. Electromagn. Compat.* **2009**, *51*, 443–452. [CrossRef]
42. Miki, M.; Miki, T.; Asakawa, A.; Shindo, T.; Yokoyama, S. Characteristics of upward leaders of winter lightning in the coastal area of the sea of Japan. *IEEJ Trans. Power Energy* **2012**, *132*, 560–567. [CrossRef]
43. Shindo, T.; Miki, M.; Asakawa, A. Lightning protection of wind turbines against winter lightning in Japan. In Proceedings of the International Conference on Lightning Protection, Vienna, Austria, 16–20 September 2012; pp. 1–4.
44. Zhang, M.; Li, Q.; Li, H.; Yu, W.; Guo, Z.; Siew, W.H. Damage Mechanism of Wind Turbine Blade under the Impact of Lightning Induced Arcs. *J. Renew. Sustain. Energy* **2019**, *11*, 053306. [CrossRef]
45. Vasa, N.J. Experimental study on lightning attachment manner considering various types of lightning protection measures on wind turbine blades. In Proceedings of the 28th International Conference on Lightning Protection (ICLP2006), Kanazawa, Japan, 17–21 September 2006; pp. 1483–1487.

46. Arinaga, S. Experimental Study on Lightning Protection Methods for Wind Turbine Blades. In Proceedings of the 28th International Conference on Lightning Protection (ICLP2006), Kanazawa, Japan, 11–21 September 2006; pp. 1493–1496.
47. Yokoyama, S. Lightning protection of wind turbine blades. *Electr. Power Syst. Res.* **2013**, *94*, 3–9. [CrossRef]
48. Montanyà, J.; March, V.; Hermoso, B.; Hermoso, J. High-speed videos of laboratory leaders emerging from wind turbine blade tips. In Proceedings of the 30th Lightning Protection (ICLP2010), Cagliari, Italy, 13–17 September 2010; pp. 1–5.
49. Muto, A.; Suzuki, J.; Ueda, T. Performance comparison of wind turbine blade receptor for lightning protection. In Proceedings of the 30th Lightning Protection (ICLP2010), Cagliari, Italy, 13–17 September 2010; pp. 1–6.
50. Abd-Elhady, A.M.; Sabiha, N.A.; Izzularab, M.A. Experimental evaluation of air-termination systems for wind turbine blades. *Electr. Power Syst. Res.* **2014**, *107*, 133–143. [CrossRef]
51. Guo, Z.; Li, Q.; Ma, Y.; Ren, H.; Fang, Z.; Chen, C.; Siew, W.H. Experimental study on lightning attachment manner to wind turbine blades with lightning protection system. *IEEE Trans. Plasma. Sci.* **2019**, *47*, 635–646. [CrossRef]
52. Radičević, B.M.; Savić, M.S.; Madsen, S.F.; Badea, I. Impact of wind turbine blade rotation on the lightning strike incidence—A theoretical and experimental study using a reduced-size model. *Energy* **2012**, *45*, 644–654. [CrossRef]
53. Guo, Z.; Li, Q.; Yu, W.; Arif, W.; Siew, W.H. Experimental study on lightning attachment manner to rotation wind turbine blade. In Proceedings of the 34th International Conference on Lightning Protection (ICLP2018), Rzeszow, Poland, 2–7 September 2018; pp. 1–5.
54. Wen, X.; Deng, Y.; Wang, Y.; Lan, L.; Qu, L.; Wang, J.; Wang, H. Discharge path observation and the statistical characteristics of discharge paths for long–air gap discharge for in-operation wind turbines. *Wind Energy* **2020**, *23*, 1351–1366. [CrossRef]
55. Minowa, M.; Ito, K.; Sumi, S.I.; Horii, K. A study of lightning protection for wind turbine blade by using creeping discharge characteristics. In Proceedings of the 31st Lightning Protection (ICLP2012), Vienna, Austria, 2–7 September 2012; pp. 1–4.
56. Wu, Q.; Yang, Q. Scaled experiment and observation of the lightning discharge process of rotating wind turbines under different shapes of high-voltage electrodes in the laboratory. *Electr. Power Syst. Res.* **2024**, *231*, 110339. [CrossRef]
57. Wen, X.; Qu, L.; Wang, Y.; Si, T.; Xu, J.; Lan, L. Experimental Study of the Influence of the Blade Rotation on Triggered Lightning Ability of Wind Turbine's Blades. *Proc. CSEE* **2017**, *37*, 2151–2159. (In Chinese)
58. He, T.; He, H.; Shi, W.; Zhang, Z.; Yin, Y.; Chen, W. Experimental Study on the GFRP Laminate Breakdown of Wind Turbine Blades due to Lightning Strikes by using Long Sparks. In Proceedings of the 2017 International Conference on Lightning and Static Electricity, Nagoya, Japan, 13–15 September 2017; p. 3C3-8.
59. He, H.; Chen, W.; Luo, B.; Bian, K.; Xiang, N.; Yin, Y.; Zhang, Z.; Dai, M.; He, T. On the electrical breakdown of GFRP wind turbine blades due to direct lightning strokes. *Renew Energy* **2022**, *186*, 974–985. [CrossRef]
60. Jiang, L.; Jiang, Z.; Lu, J.; Hu, D.; Xie, P.; Huang, X. Accumulation characteristics of precipitation static on rotating wind turbine blades and its influence on the lightning attachment characteristics. *High Volt.* **2024**, *9*, 1270–1279. [CrossRef]
61. Li, X.; Li, X.; Mu, Z.; Li, Y.; Feng, F. An Experimental Study on Biochar/Polypyrrole Coating for Blade Anti-Icing of Wind Turbines. *Coatings* **2023**, *13*, 759. [CrossRef]
62. Golde, R.H. The Lightning Conductor. *J. Frankl. I.* **1967**, *283*, 451–463. [CrossRef]
63. Eriksson, A.J. An Improved Electrogeometric Model for Transmission Line Shielding Analysis. *IEEE Trans. Power Deliv.* **1987**, *2*, 871–886. [CrossRef]
64. Rizk, F. A model for switching impulse leader inception and breakdown of long air-gaps. *IEEE Trans. Power Deliv.* **1989**, *4*, 596–603. [CrossRef]
65. Goelian, N.; Lalande, P.; Bondiou-Clergerie, A.; Bacchiega, G.L.; Gazzani, A.; Gallimberti, I. A simplified model for the simulation of positive-spark development in long air gaps. *J. Phys. D Appl. Phys.* **1997**, *30*, 2441–2452. [CrossRef]
66. Becerra, M.; Cooray, V. A simplified physical model to determine the lightning upward connecting leader inception. *IEEE T Power Deliv.* **2006**, *21*, 897–908. [CrossRef]
67. Golde, R.H. *Lightning Protection*; Edward Arnold: London, UK, 1973; pp. 26–30.
68. Rakov, V.A.; Lutz, A.O. A New Technique for Estimating Equivalent Attractive Radius for Downward Lightning Flashes. In Proceedings of the 20th International Conference on Lightning Protection, Interlaken, Switzerland, 24–28 September 1990; pp. 1–2.
69. Warner, T.A. Observations of simultaneous upward lightning leaders from multiple tall structures. *Atmos. Res.* **2012**, *117*, 45–54. [CrossRef]
70. Hill, J.D.; Uman, M.A.; Jordan, D.M. High-speed video observations of a lightning stepped leader. *J. Geophys. Res. Atmos.* **2011**, *27*, D16. [CrossRef]
71. Saba, M.M.F.; Paiva, A.R.; Schumann, C.; Ferro, M.A.S.; Naccarato, K.P.; Silva, J.C.O.; Custódio, D.M. Lightning attachment process to common buildings. *Geophys. Res. Lett.* **2017**, *44*, 4368–4375. [CrossRef]
72. Bazelyan, E.M.; Raizer, Y.P.; Aleksandrov, N.L. Corona initiated from grounded objects under thunderstorm conditions and its influence on lightning attachment. *Plasma Sources Sci. Technol.* **2008**, *17*, 024015. [CrossRef]
73. Becerra, M. Glow corona generation and streamer inception at the tip of grounded objects during thunderstorms: Revisited. *J. Phys. D Appl. Phys.* **2013**, *46*, 135205. [CrossRef]

74. Becerra, M. Corona discharges and their effect on lightning attachment revisited: Upward leader initiation and downward leader interception. *Atmos. Res.* **2014**, *149*, 316–323. [CrossRef]
75. Wang, D.; Takagi, N. Characteristics of winter lightning that occurred on a windmill and its lightning protection tower in Japan. *IEEJ Trans. Power Energy* **2012**, *132*, 568–572. [CrossRef]
76. Yu, W.; Li, Q.; Zhao, J.; Li, H.; Siew, W.H. Thundercloud-Induced Spatial Ion Flow in the Neighborhood of Rotating Wind Turbine and Impact Mechanism on Corona Inception. *IEEE Trans. Plasma. Sci.* **2021**, *49*, 2925–2935. [CrossRef]

Disclaimer/Publisher's Note: The statements, opinions and data contained in all publications are solely those of the individual author(s) and contributor(s) and not of MDPI and/or the editor(s). MDPI and/or the editor(s) disclaim responsibility for any injury to people or property resulting from any ideas, methods, instructions or products referred to in the content.